39. Marset, D., Dolza, C., Boronat, T., Montanes, N., Balart, R., Sanchez-Nacher, L., Quiles-Carrillo, L. (2020). Injection-Molded Parts of Partially Biobased Polyamide 610 and Biobased Halloysite Nanotubes. Polymers, 12 (7), 1503. doi: https://doi.org/10.3390/polym12071503
40. Kamerling, S., Schlarb, A. K. (2020). Magnesium hydroxide – A new lever for increasing the performance and reliability of PA66/steel tribosystems. Tribology International, 147, 106271. doi: https://doi.org/10.1016/j.triboint.2020.106271

Fluorine-doped tin oxide (FTO) thin films have been deposited by the modified spin coating method at 3000 rpm using tin (II) chloride dehydrate ($SnCl_2{\cdot}2H_2O$) as a precursor, ammonium fluoride (NH4F) as a dopant and ethanol as a solvent. The aim of this research is to find out the quality of the thin film based on the number of cycles (3, 4, 5, and 6 cycles) and annealing temperature (300, 400 and 500 °C). The variation of annealing temperature and number of cycles can affect the crystal structure of the FTO thin film, crystal size and grain size. Increasing the number of cycles and annealing temperature can lead to larger crystallite size and lower dislocation density, so that electrons between the grains can move easily. The large grain can reduce the grain boundary, increasing the electron mobility and decreasing the resistivity. XRD analysis shows that the structure of SnO_2 polycrystalline with the most dominant crystal plane (110) is formed in this research when compared to the intensity of other structures. The resistivity value decreases with increasing the annealing temperature and number of cycles. In addition, transparency value also decreases along with increasing the annealing temperature and number of cycles. The optimum results of resistivity and transparency values obtained in this research are $1.69{\times}210^{-2}$ Ω·cm and 69.232 % at 500 °C and 5 cycles. These results can be used as a reference for further study to optimize the production of fluorine-doped tin oxide (FTO) thin film with spin coating. Therefore, many factors that affect the production of fluorine-doped tin oxide (FTO) thin film, either dissolving stage or deposition process on the substrate surface still need to be studied deeply to obtain the optimum result

Keywords: spin coating, number of cycles, annealing temperature, resistivity, transmittance

UDC 621.793
DOI: 10.15587/1729-4061.2020.210818

CONTROLLER OF FLUORINE-DOPED TIN OXIDE THIN FILMS DEPOSITION VIA CYCLES AND ANNEALING TEMPERATURES BY SPIN COATING TECHNIQUES

Tri Arini
Master of Engineering, Junior Researcher*
E-mail: arinitri82@gmail.com
Latifa Hanum Lalasari
Doctor of Engineering, Senior Researcher*
Lia Andriyah
Master of Physical and Mathematical Sciences, Junior Researcher*
Nadia Chrisayu Natasha
Master of Engineering, Junior Researcher*
Fariza Eka Yunita
Master of Engineering, Junior Researcher*
Florentinus Firdiyono
Doctor of Engineering, Professor*
Adjie Syaputra
Bachelor of Engineering, Undergraduate Student***
Amalia Sholehah
Doctor of Engineering, Associate Professor***
Achmad Subhan
Master of Engineering, Senior Researcher
Research Center for Physics**
Indonesian Institute of Sciences (LIPI)
Kawasan Puspiptek Serpong, Tangerang Selatan, 15314, Indonesia
*Research Center for Metallurgy and Material**
**Indonesian Institute of Sciences (LIPI)
Building 470, Kawasan Puspiptek Serpong,
Tangerang Selatan, 15314, Indonesia
***Department of Metallurgy Engineering
Universitas Sultan Ageng Tirtayasa
Jl. Jenderal Sudirman Km 3, Kota Cilegon, Banten, 42435, Indonesia

Received date 01.09.2020
Accepted date 12.10.2020
Published date 30.10.2020

1. Introduction

A dye-sensitized solar cell (DSSC) is a technology that converts sunlight energy (visible light) into electrical energy. One of the components that support the DSSC working process is a transparent conductive oxide (TCO). Transparent conducting oxide is a thin layer of metal oxide that has high electrical conductivity and optical transparency [1]. Besides supporting the DSSC working process, this TCO can also be applied in the daily activity such as sensors, solar

cells, batteries and touch screens. TCO has a high selling value because it has valuable functions. Currently, TCO has passed many developments in materials, manufacturing methods and applications. TCO must have good transparency and conductivity properties to fulfill its application. A good level of transparency is obtained with the amorphous structure in the material, but the crystallinity value is directly proportional to the conductivity. This causes the need in increasing the degree of crystallinity that can reduce amorphous properties to achieve optimal conductivity [2].

Currently, the most common TCO thin film commercialized by the manufacturing industry is indium tin oxide (ITO). However, ITO has disadvantages that are the raw material is very expensive and its availability is limited. Tin oxide (SnO_2) is a transparent conductive oxide that has been widely studied as a substitute for ITO. The advantage of SnO_2 is that it can withstand high temperatures and is stable chemically and mechanically [3]. An effective way to increase the electrical conductivity and optical transparency of TCO thin films is adding the doping as impurities such as antimony, fluorine, niobium and tantalum [4]. Fluorine doped tin oxide (FTO) is a transparent conductive oxide material that is widely researched as an alternative to indium tin oxide (ITO) that is cheaper [5] and the raw materials are easier to obtain.

2. Literature review and problem statement

TCO alternative studied in this research was transparent conductive glass FTO as an alternative to indium tin oxide (ITO). Various techniques can be used to synthesize oxides, particularly SnO_2, including chemical vapour deposition (CVD) [6], physical vapour deposition (PVD) [7], spray pyrolysis [8], pulsed laser deposition (PLD) [9], DC reactive sputtering [10], dip coating [11], and spin coating [12]. Doyan, et. al said that the thin layer growth of SnO_2 with fluorine doping using the spray pyrolysis method has a weakness, namely the formed layer is not homogeneous and cracks occur after heating [13]. Whereas with the sputtering method, the adhesion between the thin layer and the substrate is getting better, but requires complicated equipment [14]. Among those techniques, sol-gel spin coating has the advantage of being able to form a homogeneous film layer [14] but it has not been widely tried for the manufacture of FTO films. Therefore, in this study a research will be conducted on the manufacture of FTO thin layers by studying the effect of the number of cycles and annealing temperature.

Goebbert, et. al. in 1999 examined the wet chemical deposition of the ATO layer using the spin coating technique, $SnCl_4$ as a precursor and 5 mol % Sb as the dopant. The obtained resistivity value was 1.7×10^{-2} Ω·cm at 550 °C [15]. As we know, antimony (Sb) is one of the poisonous doping agents, so we need environmentally friendly antimony as an alternative. Based on these reasons, the present research will use fluorine doping where this doping is more environmentally friendly than antimony (Sb).

Moradi, et. al. in 2014 [16] conducted a study on the effect of solution and coating thickness on the manufacture of tin-doped indium oxide (ITO) using $SnCl_4$ as precursors, indium nitrate hydrate as dopants then using ethanol (Merck Co.) and acetyl acetone (AcAc, Merck Co., (98 %) as a variety of solvents. As we know, indium nitrate hydrate is one of the economic doping agents, so an alternative to replace indium nitrate is needed. The crystal structure obtained indicates that the crystallinity of indium oxide formed successfully. The optimum result obtained in this study is a resistivity value of 0.412×10^{-1} Ω·cm and the thickness was 165 nm with 7 layers at 550 °C. In his research, he concluded that the ethanol solvent was better than acetyl acetone. According to Moradi et al, acetyl acetone is the right agent for making transparent thin films because acetyl acetone causes the formation of smaller particles, so that the conductivity of thin films decreases. On the other hand, ethanol is a good solvent with less than 7 layers used. Unfortunately, the resistivity value obtained for the TCO thin layer is still under the 10^{-4} Ω·cm scale.

Subramanian, et. al [17] studied the effect of temperature variations on FTO thin films with the precursors $SnCl_4{\cdot}5H_2O$, F/Sn ratio 7.5 %, 3½ and 5½ days of aging, speed 3000 rpm and 10 layers. The most common precursor used in the spin coating method by previous researchers is $SnCl_4{\cdot}5H_2O$ with the oxidation number of IV, which leads to the formation of fluorine-doped tin oxide thin films and SnO_2 nanocrystals. $SnCl_2{\cdot}2H_2O$ is an alternative precursor to $SnCl_4{\cdot}5H_2O$ because $SnCl_2{\cdot}2H_2O$ can be found easily and more economically. The solution making process carried out by Subramanian requires a large amount of energy, because the solution was stirred and refluxed at 60 °C for one hour. Hence, in our research, we will try the manufacturing process at room temperature so that no temperature energy is needed in making the solution. Subramanian also used aging process for 3½ and 5½ days when making the solution. Unfortunately, the aging time will affect the viscosity value, the high viscosity value causes bad adhesion and comet formation on the coated film. That is a challenge for us not to use the aging time in the solution making process. We hope that the shorter deposition time will be able to produce the desired conductive glass layer. The result obtained by Subramanian, et. al is the minimum value of sheet resistance of 40 Ω/sq at 375 °C, but this value also does not meet the requirements for the optimum value of TCO thin film with sheet resistance on a scale of ~18 Ω/sq. The resulting film structure shows polycrystalline properties with a preferred orientation along the plane (110) at lattice constants a (4.7324 Å) and c (3.1924 Å) but the sharpness of this crystalline plane starts at 350 °C while at 325 °C crystal field sharpness does not yet appear. According to this research, the grain size increases along with increasing temperature and the average grain sizes obtained were 143.76 nm and 414.8 nm.

Another research was carried out by Kahattha, et.al [18] studied the effect of temperature annealing on the optical properties of FTO thin films with $SnCl_4{\cdot}5H_2O$ precursor, 10 % dopant concentration of NH_4F, 2-methoxyethanol and monoethanolamine (MEA), respectively used as a solvent and stabilizer. Similar to the research conducted by Subramanian, et. al, Kahatta also used 20 h of aging, a speed of 2,000 rpm and 10 layers. For the same reason, it is a challenge for the author no to do an experiment using $SnCl_2{\cdot}2H_2O$ as a precursor and the dissolving process without aging. Kahatta, et. al said that the average grain size of FTO thin films increases with increasing annealing temperature. The XRD pattern given in this research showed that at 300 °C the amorphous phase and polycrystalline phase of SnO_2 with plane peaks (110), (101) and (200) formed at 400 °C are produced. Due to the amorphous phase achieved under 300 °C, the annealing temperature that we used in this research was started at 300 °C.

3. The aim and objectives of the study

The aim of this study is to determine the quality of the FTO thin film formed based on the number of cycles (3–6 cycles) and annealing temperature at 300, 400, 500 °C.

To achieve this aim, the following objectives are accomplished:

– to study the effect of adding fluorine to a pure tin solution;

– to determine the optimum parameters for the number of cycles and annealing temperature on crystallinity, morphology, resistivity values and optical properties of FTO glass with $SnCl_2{\cdot}2H_2O$ as a precursor and NH_4F as a dopant;

– to study the correlation of annealing temperature and the number of cycles on optical properties and the value of crystallinity, morphology, and resistivity.

4. Materials and experimental method

The materials used in this study were tin (II) chloride dehydrate ($SnCl_2{\cdot}2H_2O$) (Merck®), ammonium fluoride (NH_4F) (Merck®), ethanol (Merck®) and soda-lime microscope slide glass substrates. The first step was cleaning the substrate in the same ways that were carried out by Arini, et. al. [19]. The solution was made of two types of solutions. The first solution (undoped) is a mixture of 12 grams tin (II) chloride dehydrate ($SnCl_2{\cdot}2H_2O$) with 100 ml ethanol, stirred at 3000 rpm for 30 minutes. Furthermore, the doped solution was made using the initial composition of the first solution with the addition of 0.24 grams NH_4F doping, then stirred again for 30 minutes until homogeneous.

The deposition process used the spin coating method with a fairly simple, easy and economical tool with a speed of 3,000 rpm. The solution was deposited on a surface with a height of 2 cm as much as 1 drop for 90 seconds maintained on a hot plate at 200 °C for 10 minutes. This process was repeated with the variations in the number of cycles 3, 4, 5 and 6 times. After that, the annealing process was carried out with annealing temperature variations of 300, 400, and 500 °C for 1 hour.

The crystallinity and structural properties of the SnO_2 thin films were characterized using x-ray diffraction (XRD) (Shimadzu XRD-7000). Surface morphology was characterized using the scanning electron microscope – energy dispersive spectroscopy (SEM-EDS) (JEOL-JSM 6390A), while the thickness of the SnO_2 thin layer was characterized using FE SEM (FEI INSPECT F50). The transmission and electricity spectra were characterized using UV-Vis spectroscopy (Thermo UV-Vis Genesys 10s) and four-point probe (FPP5000).

5. Results of determining the thin film quality

5. 1. Effect of the number of cycles

5. 1. 1. Crystal structure

XRD patterns of SnO_2 thin film at 500 °C and deposition of 90 seconds with the different number of cycles are shown in Fig. 1. Based on Fig. 1, crystal planes (110), (101), (200), (211), (220), and (310) indicate the formation of the tetragonal crystal structure of SnO_2 (JCPDS: 41-1445) and show polycrystalline [20].

Based on Table 1, the results of XRD characterization will get the value of Full Width Half Maximum (FWHM). Increasing the number of cycles causes a decrease in the value of FWHM at the peak (110). The FWHM values for the number of cycles 3, 4, 5 and 6 are 1.333; 0.790; 0.723 and 0.624°. This corresponds to the crystallite size that has increased with the increasing number of cycles.

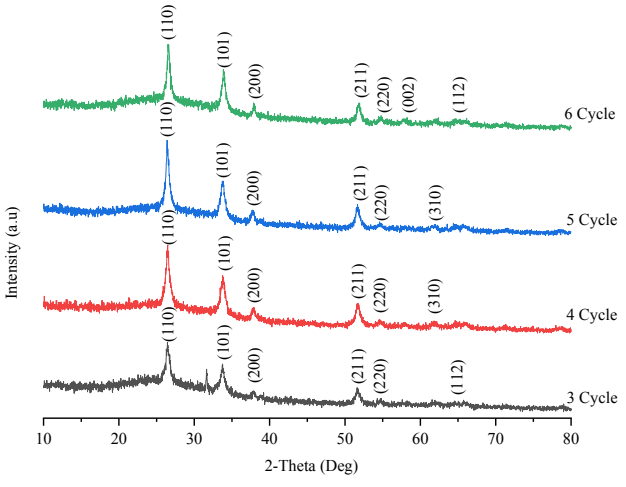

Fig. 1. XRD diffraction patterns of SnO2 thin film with the variations in the number of cycles at a deposition time of 90 seconds and annealing temperature of 500 °C

Table 1

Number of cycles effect on the characteristics of the SnO_2 thin film

Sample	HKL	2 Theta	FWHM	*D* (Å)	*D* average (Å)
3 cycles, 500 °C	110	26.454	1.333	45.138	85.461
	101	33.708	0.876	71.152	
	200	37.812	0.554	162.204	
	211	51.666	0.673	100.322	
	220	54.658	0.543	128.501	
	112	63.668	12.245	5.448	
4 cycles, 500 °C	110	26.455	0.790	78.098	96.715
	101	33.762	0.826	75.782	
	200	37.836	0.637	138.206	
	211	51.679	0.787	102.782	
	220	54.600	0.789	118.553	
	310	61.862	1.033	66.867	
5 cycles, 500 °C	110	26.430	0.723	85.871	108.832
	101	33.733	0.728	86.623	
	200	37.743	0.506	174.182	
	211	51.639	0.717	115.358	
	220	54.612	0.575	120.476	
	310	61.735	0.982	70.483	
6 cycles, 500 °C	110	26.565	0.624	100.633	111.552
	101	33.864	0.615	103.919	
	200	37.918	0.342	260.462	
	211	51.773	0.622	109.350	
	220	54.755	0.809	83.518	
	002	57.756	0.637	109.525	
	112	64.553	5.009	13.461	

The crystallite size in each cycles can be seen in Table 1. Table 1 shows that the smallest crystallite size was obtained when the number of cycles was 3, namely 85.461 Å. The value of the largest crystallite size was obtained when the number of cycles was 6, namely 111.552 Å.

5. 1. 2. Surface morphology

The morphology of the FTO thin film was observed in the SEM images (Fig. 2). Fig. 2 shows the FTO thin films with 3, 4, 5 and 6 cycles. Increasing the number of layers from 3 to 6 will cause an increase in the number of grains and the empty spots will be filled, thus the grain size will be bigger.

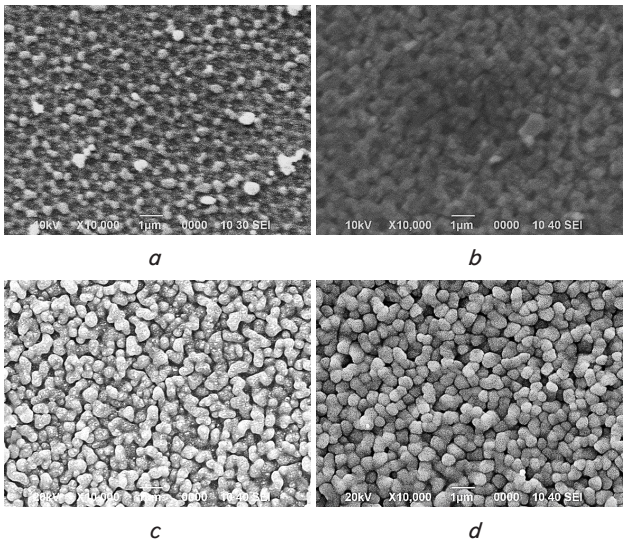

Fig. 2. Morphology of the SnO_2 thin layer at 500 °C for 90 seconds with variations in the number of cycles: *a* — 3 cycles; *b* — 4 cycles; *c* — 5 cycles; *d* — 6 cycles

Fig. 2, *a* shows that small grains start to form and there are voids between the grains (dark appearance). Based on Fig. 2, *b–d*, with increasing the number of cycles to 4, 5 and 6, the grain size will be bigger, with an average size of 292.08; 453.82 and 469.57 nm, respectively.

5. 1. 3. Properties of electricity

Table 2 is the measurement result of the resistivity of the SnO_2 thin layer with a variation in the number of cycles. The resistivity values of 3, 4, 5 and 6 cycles are 1.468×10^{-1} Ω·cm, 0.368×10^{-1} Ω·cm, 1.692×10^{-2} Ω·cm and 0.854×10^{-2} Ω·cm, respectively.

Table 2

Resistivity value of the SnO_2 thin film with a variation in the number of cycles, fixed deposition 90 seconds and 500 °C

Sample	Resistivity (Ω·cm)
3 cycles	1.468×10^{-1}
4 cycles	0.368×10^{-1}
5 cycles	1.692×10^{-2}
6 cycles	0.854×10^{-2}

From Table 2, it can be seen that there is a downward trend in the resistivity value along with increasing the number of cycles, which means that the conductivity will increase with increasing the number of cycles.

5. 1. 4. Optical properties

The optical properties of the SnO_2 thin film were characterized by measuring the optical transmittance spectrum (T) in the 300–800 nm range. The layer was deposited at 3,000 rpm for 90 seconds with 3, 4, 5 and 6 cycles. The transmittance value of the SnO_2 thin layer can be seen in Fig. 3.

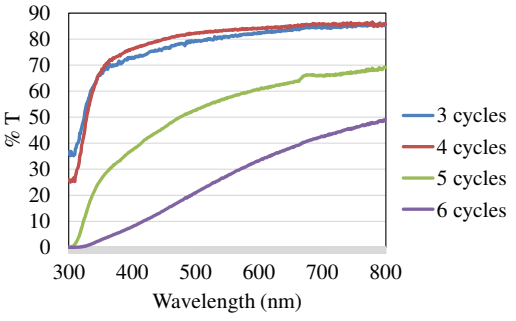

Fig. 3. Transmittance value of the SnO_2 thin film with a variation in the number of cycles, fixed deposition 90 seconds and 500 °C

With the number of cycles 3 and 4, the thin layer still looks transparent with a transmittance value of 85.897 and 85.264 %. The transmittance value has decreased sharply with an increase in the number of cycles to 5 and 6 (69.232 and 49.078 %).

5. 2. Effect of doping and annealing temperature

5. 2. 1. Crystal structure

XRD diffraction patterns of the SnO_2 thin film with a variation of annealing temperature, fixed deposition of 90 seconds, number of cycles of 5 are shown in Fig. 4. In this deposition process, a comparison will be made between the 2 wt % doped and undoped samples to know the effect of giving fluorine as doping. The XRD analysis shows that the peaks indicate the phase of SnO_2 material with crystal planes (110), (101), (200), (211), (220), and (310), which show the tetragonal crystal structure of SnO_2 (JCPDS: 41-1445) [20].

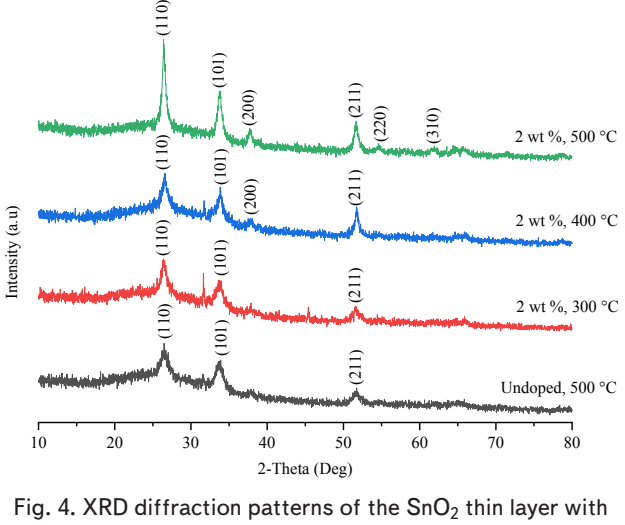

Fig. 4. XRD diffraction patterns of the SnO_2 thin layer with annealing temperature variation, fixed deposition 90 seconds, 5 cycles

From Table 3, it can be seen that when the annealing temperature increases from 300 to 500 °C, the FWHM value in the crystal plane (110) tends to decrease, namely 2.078, 1.626 and 0.723°. The trend of these FWHM values indicates that the crystallinity of the SnO_2 film increases due to the increased annealing temperature [21].

Table 3

Effect of annealing and doping temperatures on the results of XRD characterization of the SnO_2 thin film

Sample	HKL	2 Theta	FWHM	*D* (Å)	*D* average (Å)
undoped, 500 °C	110	26.447	3.098	19.013	38.947
	101	33.678	1.502	40.559	
	211	51.707	1.552	57.269	
2 % wt, 300 °C	110	26.454	2.078	28.567	50.376
	101	33.675	1.342	45.564	
	211	51.643	0.927	76.997	
2 % wt, 400 °C	110	26.534	1.626	36.751	92.269
	101	33.806	0.917	67.840	
	200	37.854	0.693	126.536	
	211	51.705	0.503	137.951	
2 % wt, 500 °C	110	26.430	0.723	85.871	108.832
	101	33.733	0.728	86.623	
	200	37.743	0.506	174.182	
	211	51.639	0.717	115.358	
	220	54.612	0.575	120.476	
	310	61.735	0.982	70.483	

According to Table 3, the size of crystals formed in the undoped sample is 38.947 Å, while the size of the 2 wt % doped crystallite at annealing temperatures of 300, 400 and 500 °C is 50.376; 92.269 and 108.832 Å.

5. 2. 2. Surface morphology

SEM images of FTO thin films coated with variations in annealing temperature, fixed deposition 90 seconds, number of layers 5 are shown in Fig. 5. Fig. 5, *a* shows the morphology of undoped thin films with small grain sizes and not dense, there are voids between the grains (dark appearance) thereby reducing the conductivity of the sample [22].

With the addition of 2 wt % doping, there was a change in the morphology of the thin film. The surface morphology of the FTO thin film with a flat and smooth surface consisting of small fine grains appears at 300 °C. Whereas at 500 °C, FTO thin films show a rougher surface and larger grain size than FTO thin films annealed at 300 and 400 °C with average sizes of 56.41; 183.22 and 469.57 nm.

The thickness of the SnO_2 thin film annealed at 500 °C can be seen from the cross-sectional FE-SEM shown in Fig. 5, *e*. The transverse images of FE SEM show a fairly even and uniform thickness with the estimated thin film thickness about 0.83 μm. In addition, it is also seen that the thin film has a sharp interface between the substrate and the SnO_2 thin film (Fig. 5, *e*).

5. 2. 3. Properties of electricity

Table 4 is the measurement result of the resistivity of the SnO_2 thin film with the variations in annealing temperature. Based on Table 4, the resistivity value decreased with increasing the annealing temperature in the 2 % wt doped sample. The resistivity value decreased from 4.08×10^{-1} to 1.69×10^{-2} Ω·cm when the annealing temperature increased from 300 to 500 °C. The resistivity value of the undoped thin film at 500 °C is 1.82×10^{0} Ω·cm, which is higher than for samples using doping.

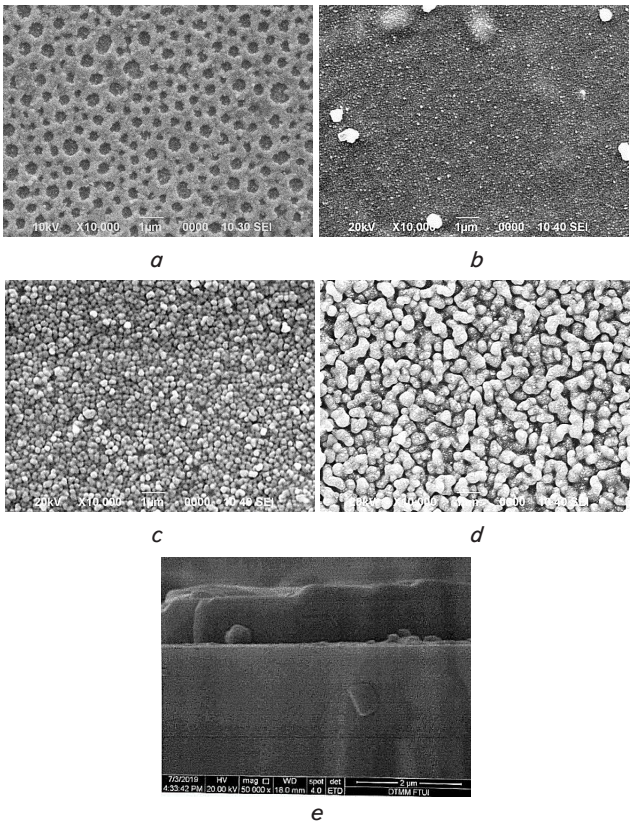

Fig. 5. Morphology of the SnO_2 thin film with variations in substrate temperature, fixed deposition 90 seconds, 5 cycles: *a* – undoped at 500 °C, *b* – 2 wt % doped at 300 °C; *c* – 2 wt % doped at 400 °C; *d* – 2 wt % doped at 500 °C, *e* – cross-sectional view with 2 wt % doped at 500 °C

Table 4

Resistivity value of the SnO_2 thin layer with annealing temperature variations, fixed deposition 90 seconds, 5 cycles

Sample	Resistivity (Ω·cm)
2 wt % doped, 300 °C	4.080×10^{-1}
2 wt % doped, 400 °C	5.330×10^{-2}
2 wt % doped 500 °C	1.692×10^{-2}
undoped, 500 °C	1.821×10^{0}

Table 4 shows that the addition of dopants has an effect on the resistivity value where the addition of fluorine element as a dopant on the precursor decreases the resistivity value. This is supported by the XRD analysis (Fig. 4), which shows that increasing the amount of F doping made the FTO glass more crystalline.

5. 2. 4. Optical properties

Differentiation in the transmittance value of the SnO_2 thin film with variations in annealing temperature can be seen on the UV-Vis graph in Fig. 6. Fig. 6, *a* shows a transmittance spectrum (undoped) with a higher transmittance value (85.78 %) than for the doped sample.

The optical transmittance spectra of the FTO thin films with annealing temperatures at 300, 400 and 500 °C are shown in Fig. 3, *b, d*. The average transmission of SnO_2 thin films in the wavelength range of 300–800 nm shows a significant change with the increase of annealing temperature.

The transmittance values at 300, 400 and 500 °C were 81.72; 77 and 69.23 %.

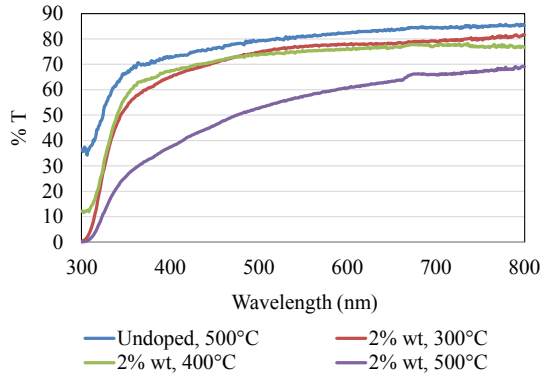

Fig. 6. Transmittance value of the SnO_2 thin film with a variation in the annealing temperature, fixed deposition 90 seconds, 5 cycles

6. Discussion of results

6. 1. Discussion of results of the effect of the number of cycles

Based on Fig. 1, crystal planes (110), (101), (200), (211), (220), (310) and (301) indicate the formation of the tetragonal crystal structure of SnO_2 (JCPDS: 41-1445) and show polycrystalline [20]. The crystal plane 110 has the most dominant structure in all cycle variables compared to other crystal planes. This is caused by a phenomenon related to the growth of nucleation on the surface [17]. Besides that, other crystal planes are formed, namely the crystal fields (101), (200) and (211), but with lower intensities. Crystal fields (220), (002), (310), (112) are additional peaks that arise due to variations in the number of cycles where the increasing number of cycles makes the peak intensity of each peak relatively increased. The peak intensity of XRD increases with the number of cycles, this is supported by a research conducted by Dissanayake, et al in 2018 [23]. Crystallinity of thin films increases with increasing the number of cycles. This is indicated by the intensity and sharpness of XRD peaks of the SnO_2 thin film [24] as in Fig. 1.

In this study, the crystallite size value increases due to the decrease in the value of FWHM. It corresponds to Scherrer's equation [25].

$$t=\frac{k\lambda}{\beta\cos\Theta}, \quad (1)$$

where t is the size of crystallite diameter, k is the proportionality constant (0.9), λ is the wavelength of X-ray diffraction used (1.54 Å), β is FWHM, and θ is the Bragg diffraction angle. According to the crystalline size data shown in Table 1, it can be concluded that the greater the number of cycles, the higher the crystalline size. The degree of crystallinity and intensity of the crystalline plane increased due to the increase in the number of cycles on the SnO_2 thin film surface [24].

Based on Fig. 2, *b–d*, with the increase in the number of cycles to 4, 5 and 6, the grain size is getting bigger, this is consistent with the research conducted by SN Sadikin who said that samples with a higher number of spin coatings cause the grain size to be larger at the highest spin layer and the layer thickness will also increase with the increase in the number of cycles [26]. The research result shows that the number of cycles has a significant effect on the increase in the grain size of the FTO thin film. This corresponds to the XRD analysis in Fig. 1.

Table 2 shows that the resistivity value decreases with increasing the number of cycles. Therefore, the film conductivity will increase. This is supported by the XRD diffraction patterns formed in Fig. 1. In the XRD analysis, the crystallite size increases with increasing the number of cycles where the large crystallite size reduces the dislocation density. Hence, the electrons between the grains are easily transferred. The large grain size reduces the grain boundaries that increase the mobility of the electrons and consequently the resistivity of the film decreases [12].

The transmittance value of the SnO_2 thin film in Fig. 3 indicates that as the number of cycles increases, the transmittance value decreases. This is caused by the strong absorption power of the SnO_2 thin film and its absorption spectrum. The transmittance decreases as the number of cycles increases due to the increasing film thickness and then continues at a higher wavelength region [23]. This is supported by the previous research conducted by A. Kocygit, et al., who stated that the layer thickness increases linearly with the increasing number of layers but will cause optical properties (transmittance) to decrease [24]. Based on Fig. 3, the optimum condition for obtaining a high transmittance value is when the number of cycles is 3.

6. 2. Discussion of results of doping and annealing temperature

In Fig. 4, it can be seen that in the undoped glass film of SnO_2, the formed crystal planes are (110), (101) and (211) and the intensity in each crystal plane is still low. The intensity of each peak will increase with the increase in the *F* doping amount. It indicates that the addition of the *F* doping element will affect the resulting SnO_2 crystal shape. Besides that, it can also be seen from the XRD diffraction pattern that the crystallinity value increases significantly when comparing doped to undoped samples. Thus, it can be concluded that *F* doping will increase the crystallinity of the SnO_2 thin film structure.

The crystal plane in Fig. 4 shows polycrystalline, with the crystal plane (110) being predominant. This is supported by the research conducted by I. Y. Y. Bu, et al in 2014 who examined sol-gel deposition from FTO glass used for DSSC where the crystal structure obtained was SnO_2 with tetragonal form and the highest peak intensity in the crystal plane was (110) [27]. Amel Adjimi, et al in 2018 [28] said that the crystal plane (110) remains the orientation in research using SnO_2 or undoped. Also, crystal planes (101) and (211) are also formed with relatively lower intensity. At annealing temperatures of 400 and 500 °C, a crystalline field (200) was seen. Whereas the crystalline fields (220) and (301) formed only at 500 °C. This is probably due to the increase in grain growth that will occur when the annealing temperature is raised. The increase in grain size is assumed to be related to the increase in the grain growth rate and crystal size due to a rapid increase in adsorption and diffusion rate of atoms with temperature [17].

Table 3 shows that with the addition of 2 wt % doping, the crystal size of the FTO thin films was greater when compared to the thin films that were not doped. This proves that

adding the *F* ion can increase the crystal size of SnO_2. This trend is consistent with the research that has been done by Mientus et al and Banyamin et al, who stated that grain size has increased by 5.3 %. This enlargement is due to the insertion of *F* atoms in the SnO_2 lattice, which causes stress in the lattice [29]. From Table 3, it can also be seen that the crystal size increases with increasing the annealing temperature because the annealing temperature-induced coalescence of small grains by grain boundary diffusion leads to major grain growth [18].

Fig. 5 shows the morphology of undoped thin films with small grain sizes and not dense, there are voids between the grains (dark appearance) thereby reducing the conductivity of the sample [22]. Large grain boundaries will absorb more heat and hold moving electrons, thus reducing the conductivity of a material.

With the addition of 2 wt % doping, there was a change in the thin film morphology. The surface morphology of the FTO thin film with a flat and smooth surface consisting of small fine grains formed at 300 °C. Whereas with annealing temperature at 500 °C, FTO thin films showed a rougher surface and larger grain size than FTO thin films annealed at 300 and 400 °C. Thus, the annealing temperature has a significant effect on the change in grain size of the SnO_2 thin layer, namely the grain size becomes larger with increasing the annealing temperature [30].

Atoms gain a greater diffusion activation energy at higher annealing temperatures, which allows atoms with lower surface energy to move to the energetic sites in the crystal lattice [21]. The crystallite then grows in the direction of growth at higher temperatures, thereby increasing the crystallinity of the SnO_2 thin film. This will then be followed by the incorporation of crystallite processes, forming larger granules and minimizing oxygen defects at grain boundaries [31]. The results of this morphological image are interpreted with XRD results obtained in Fig. 4.

The resistivity value decreased when the annealing temperature increased from 300 to 500 °C. This is caused by the fact that, during the annealing process, the layers receive more energy for crystal growth, which leads to an increase in particle size, a reduction in porosity or grain boundaries and possibly a decrease in electron scattering at the grain boundaries [32, 33]. In their research, Luangchaisri, et. al. said that the resistivity decreases with increasing the annealing temperature due to the increase in charge mobility so that the crystallinity becomes higher [34].

The resistivity value of the undoped thin film at 500 °C looks bigger when compared to samples using doping. The resistivity of the SnO_2 thin film decreases with increasing F/Sn atomic ratio, because fluorine doping produces free electrons through the substitution of F^- to the O site. Each F^- anion replaces the O^{-2} anion and the O^{-2} anion being replaced produces more free electrons and this will likely result in the increase in free electrons and the decrease in the resistivity value [35]. The resistivity decreases due to increased electron scattering by excess free electrons and ionized impurities [36]. This scattering mechanism affects the electrical properties and increases the resistivity of the film. In the research of S. C. Ray, et al. in 1997 using the chemical vapor deposition technique, it is said that with a decrease in grain size, the potential for grain boundaries would increase, causing an increase in the grain boundary spread and a corresponding increase in resistivity [37].

Fig. 6, *a* shows a transmittance spectrum (undoped) with a higher transmittance value than for the doped sample. It is shown that the addition of doping ions results in a decrease in transmittance value. The decrease in optical transmittance with the addition of the F/Sn ratio can be attributed to the increase in film thickness and excess free electrons in the film [36].

From Fig. 6, it can be seen that the annealing temperature has an important role in the transmittance value because the crystallinity will be better with increasing the annealing temperature [30] but reduces light scattering in the thin film. This is caused by the scattering effect increase due to large grain size and crystal aggregates, so the film thickness increases and oxygen depletion in large amounts [17]. This is similar to the previous research conducted by Sekhar C, et al in 1997 who said that the decrease in the transmittance value was caused by an increase in the surface roughness of the film, which had low sheet resistance with high thickness [37].

Fluorine-doped tin oxide thin film produced in this study has a potential for further development because it still does not meet the requirements for making transparent conductive glass (TCO) with a resistivity scale of 10^{-4} Ω·cm and a transmission value of 8085 %. However, this research can be used as a basic reference for the next FTO thin layer production using the spin coating method. Wherein this study is only limited to variations in the number of cycles and temperatures using $SnCl_2{\cdot}2H_2O$ as a precursor and ethanol as a solvent. In addition, this study has a simple and economical tool that obtained a good result but further research is still needed. Adding the vacuum into the tool to see the optimal capabilities of this FTO can be an alternative way to develop this research.

7. Conclusions

1. A prototype of transparent conductive fluorine-doped tin oxide (FTO) from the precursor $SnCl_2{\cdot}2H_2O$ tin chloride using the spin coating method with a simple and economical tool that has been modified to get pretty good results has been fabricated. The addition of fluorine ions to the Sn precursor solution was shown to improve the properties of thin films (crystallinity, crystallite size, grain size, electrical and optical properties).

2. Fluorine-doped tin oxide thin films with a variation in the number of cycles (3, 4, 5 and 6 cycles) and annealing temperature at 500 °C produced a diffraction peak that has the same characteristic as the SnO_2 diffraction pattern with the intensity in the dominant crystal plane at (110). The grain sizes for the number of cycles 4, 5 and 6 were 292.08; 453.82 and 469.57 nm, respectively. This large grain size will reduce the dislocation densities; therefore, the electrons between the grains are easily transferred then reduced the film resistivity (1.468×10^{-1}; 0.368×10^{-1}; 1.692×10^{-2} and 0.854×10^{-2} Ω·cm) and decreased the transmittance value (85.897; 85.264 %; 69.232 and 49.078 %). It is shown that increasing the number of cycles causes a decrease in resistivity and transmittance values.

Based on the obtained results, the optimum values of this research were 453.82 nm for grain size, 1.692×10^{-2} Ω·cm for resistivity value and 69.232 % for transmittance value while the number of cycles was 5, annealing temperature was 500 °C with the doped sample.

3. Fluorine-doped tin oxide thin films with various annealing temperatures (300, 400 and 500 °C) produced a phase of SnO_2 material with crystalline planes (110), (101), (200), (211), (220), (310) and tetragonal crystal structure. The grain size of SnO_2 grew bigger (56.41; 183.22 and 469.57 nm) and got denser. This reduces porosity, which causes the resistivity value to become smaller (4.080×10^{-1}; 5.330×10^{-2} and 1.692×10^{-2} Ω·cm) and decreases the transmittance value (81.72; 77 and 69.23 %). It is shown that the increase in annealing temperature results in a decrease in the resistivity and transmittance values.

Acknowledgments

The authors are grateful for the financial support of the Tematik Grant from the Research Center for Metallurgy and Materials LIPI.

References

1. Stadler, A. (2012). Transparent Conducting Oxides – An Up-To-Date Overview. Materials, 5 (12), 661–683. doi: https://doi.org/10.3390/ma5040661
2. Morris, G. C., McElnea, A. E. (1996). Fluorine doped tin oxide films from spray pyrolysis of stannous fluoride solutions. Applied Surface Science, 92, 167–170. doi: https://doi.org/10.1016/0169-4332(95)00224-3
3. Moataz, B. S., Mohamed, B. S., Sherif, A. K., Marwa, A. (2016). Preparation and Characterization of Fluorine Tin Oxide Using New Approach of Spray Technique and Electro Spinning Technique. International Journal of Advances in Science Engineering and Technology, 4 (4), 78–81.
4. Afre, R. A., Sharma, N., Sharon, M., Sharon, M. (2018). Transparent Conducting Oxide Films for Various Applications: A Review. REVIEWS ON ADVANCED MATERIALS SCIENCE, 53 (1), 79–89. doi: https://doi.org/10.1515/rams-2018-0006
5. Zahid, R., Aris, D., Kosim (2018). Preliminary Study Flourine Tin Oxide (FTO) Using Sol-Gel Spin Coating Techniques. IOSR Journal of Applied Physics (IOSR-JAP), 10 (2), 27–30.
6. Shi, X. H., Xu, K. J. (2017). Properties of fluorine-doped tin oxide films prepared by an improved sol-gel process. Materials Science in Semiconductor Processing, 58, 1–7. doi: https://doi.org/10.1016/j.mssp.2016.09.038
7. George, A., Kumari, P., Soin, N., Roy, S. S., McLaughlin, J. A. (2010). Microstructure and field emission characteristics of ZnO nanoneedles grown by physical vapor deposition. Materials Chemistry and Physics, 123 (2-3), 634–638. doi: https://doi.org/10.1016/j.matchemphys.2010.05.029
8. Agbim, E. G., Ikhioya, I. L., Ekpunobi, A. J. (2019). Syntheses and Characterization of Fluorine Doped Tin Oxide Using Spray Pyrolysis Technique. IOSR Journal of Applied Physics (IOSR-JAP), 11 (3), 70–78.
9. Yu, S., Zhang, W., Li, L., Xu, D., Dong, H., Jin, Y. (2013). Fabrication of p-type SnO_2 films via pulsed laser deposition method by using Sb as dopant. Applied Surface Science, 286, 417–420. doi: https://doi.org/10.1016/j.apsusc.2013.09.107
10. Brousseau, J.-L., Bourque, H., Tessier, A., Leblanc, R. M. (1997). Electrical properties and topography of SnO2 thin films prepared by reactive sputtering. Applied Surface Science, 108 (3), 351–358. doi: https://doi.org/10.1016/s0169-4332(96)00679-4
11. Hammad, T. M., Hejazy, N. K. (2011). Structural, electrical and optical properties of ATO thin films fabricated by dip coating method. International Journal of Material Science Innovations, 7 (4), 209–212.
12. Khan, M. I., Bhatti, K. A., Qindeel, R., Althobaiti, H. S., Alonizan, N. (2017). Structural, electrical and optical properties of multilayer TiO2 thin films deposited by sol–gel spin coating. Results in Physics, 7, 1437–1439. doi: https://doi.org/10.1016/j.rinp.2017.03.023
13. Susilawati, Doyan, A., Muliyadi, L., Hakim, S., Taufik, M., Nazarudin. (2019). Characteristics and Optical Properties of Fluorine Doped SnO_2 Thin Film Prepared by a Sol–Gel Spin Coating. Journal of Physics: Conference Series, 1397, 012003. doi: https://doi.org/10.1088/1742-6596/1397/1/012003
14. Imawanti, Y. D., Doyan, A., Gunawan, E. R. (2017). Sintesis lapisan tipis (thin film) SnO_2 dan SnO_2:Al menggunakan teknik sol-gel spin coating pada substrat kaca dan quartz. Jurnal Penelitian Pendidikan IPA, 3 (1). doi: https://doi.org/10.29303/jppipa.v3i1.49
15. Goebbert, C., Nonninger, R., Aegerter, M. A., Schmidt, H. (1999). Wet chemical deposition of ATO and ITO coatings using crystalline nanoparticles redispersable in solutions. Thin Solid Films, 351 (1-2), 79–84. doi: https://doi.org/10.1016/s0040-6090(99)00209-6
16. Moradi-Haji Jafan, M., Zamani-Meymian, M.-R., Rahimi, R., Rabbani, M. (2014). The effect of solvents and the thickness on structural, optical and electrical properties of ITO thin films prepared by a sol–gel spin-coating process. Journal of Nanostructure in Chemistry, 4 (1). doi: https://doi.org/10.1007/s40097-014-0089-y
17. Subramanian, N. S., Savarimuthu, E., Sanjeeviraja, C., Ramamurthy, S. (2005). Effect of heat treatment temperature on the spin coated fluorine doped tin oxide thin films for solar cell applications. Transactions-society for the advancement of electrochemical science and technology, 40 (2), 62–67.
18. Kahattha, C., Noonuruk, R., Pecharapa, W. (2016). Influence of annealing temperature on optical properties of fluoride doped tin oxide films grown by the sol-gel spin-coating method. Integrated Ferroelectrics, 175 (1), 138–145. doi: https://doi.org/10.1080/10584587.2016.1203646
19. Arini, T., Yuwono, A. H., Lalasari, L. H., Sofyan, N., Ramahdita, G., Firdiyono, F. et. al. (2016). The Influence of Deposition Time and Substrate Temperature during the Spray Pyrolysis Process on the Electrical Resistivity and Optical Transmittance of 2 wt% Fluorine-doped Tin Oxide Conducting Glass. International Journal of Technology, 7 (8), 1335. doi: https://doi.org/10.14716/ijtech.v7i8.7065

20. Tran, Q.-P., Fang, J.-S., Chin, T.-S. (2015). Properties of fluorine-doped SnO_2 thin films by a green sol–gel method. Materials Science in Semiconductor Processing, 40, 664–669. doi: https://doi.org/10.1016/j.mssp.2015.07.047
21. Sengupta, J., Sahoo, R. K., Bardhan, K. K., Mukherjee, C. D. (2011). Influence of annealing temperature on the structural, topographical and optical properties of sol–gel derived ZnO thin films. Materials Letters, 65 (17-18), 2572–2574. doi: https://doi.org/10.1016/j.matlet.2011.06.021
22. Trisdianto, C. A., Yuwono, A. H., Arini, T., Sofyan, N., Fikri, D., Lalasari, L. H. (2016). Optical Transmittance, Electrical Resistivity and Microstructural Characteristics of Undoped and Fluorine-doped Tin Oxide Conductive Glass Fabricated by Spray Pyrolysis Technique with Modified Ultrasonic Nebulizer. International Journal of Technology, 7 (8), 1316. doi: https://doi.org/10.14716/ijtech.v7i8.6885
23. Dissanayake, D., Samarasekara, P. Effect of number of layers on structural and optical properties of spin coated CdS films. Available at: https://www.researchgate.net/profile/Charuni_Dissanayake2/publication/324492653_Effect_of_number_of_layers_on_structural_and_optical_properties_of_spin_coated_CdS_films/links/5ad3c6bfa6fdcc29357ff477/Effect-of-number-of-layers-on-structural-and-optical-properties-of-spin-coated-CdS-films.pdf
24. Koçyiğit, A., Tatar, D., Battal, A., Ertuğrul, M., Düzgün, B. (2012). Highly efficient optoelectronic properties of doubly doped SnO_2 thin film deposited by spin coating technique. Journal of Ovonic Research, 8 (6), 171–178.
25. Suryanarayana, C., Norton, M. G. (1998). X-Rays and Diffraction. X-Ray Diffraction, 3–19. doi: https://doi.org/10.1007/978-1-4899-0148-4_1
26. Sadikin, S. N., Rahman, M. Y. A., Umar, A. A., Salleh, M. M. (2017). Effect of Spin-Coating Cycle on the Properties of TiO_2 Thin Film and Performance of DSSC. International Journal of Electrochemical Science, 12, 5529–5538. doi: https://doi.org/10.20964/2017.06.57
27. Bu, I. Y. Y. (2014). Sol–gel deposition of fluorine-doped tin oxide glasses for dye sensitized solar cells. Ceramics International, 40 (1), 417–422. doi: https://doi.org/10.1016/j.ceramint.2013.06.017
28. Adjimi, A., Zeggar, M. L., Attaf, N., Aida, M. S. (2018). Fluorine-Doped Tin Oxide Thin Films Deposition by Sol-Gel Technique. Journal of Crystallization Process and Technology, 08 (04), 89–106. doi: https://doi.org/10.4236/jcpt.2018.84006
29. Banyamin, Z., Kelly, P., West, G., Boardman, J. (2014). Electrical and Optical Properties of Fluorine Doped Tin Oxide Thin Films Prepared by Magnetron Sputtering. Coatings, 4 (4), 732–746. doi: https://doi.org/10.3390/coatings4040732
30. Ng, Z.-N., Chan, K.-Y., Tohsophon, T. (2012). Effects of annealing temperature on ZnO and AZO films prepared by sol–gel technique. Applied Surface Science, 258 (24), 9604–9609. doi: https://doi.org/10.1016/j.apsusc.2012.05.156
31. Kuo, S.-Y., Chen, W.-C., Cheng, C.-P. (2006). Investigation of annealing-treatment on the optical and electrical properties of sol–gel-derived zinc oxide thin films. Superlattices and Microstructures, 39 (1-4), 162–170. doi: https://doi.org/10.1016/j.spmi.2005.08.039
32. Patil, S. L., Chougule, M. A., Pawar, S. G., Raut, B. T., Sen, S., Patil, V. B. (2011). New process for synthesis of ZnO thin films: Microstructural, optical and electrical characterization. Journal of Alloys and Compounds, 509 (41), 10055–10061. doi: https://doi.org/10.1016/j.jallcom.2011.08.030
33. Lee, S.-M., Joo, Y.-H., Kim, C.-I. (2014). Influences of film thickness and annealing temperature on properties of sol–gel derived ZnO–SnO 2 nanocomposite thin film. Applied Surface Science, 320, 494–501. doi: https://doi.org/10.1016/j.apsusc.2014.09.099
34. Luangchaisri, C., Dumrongrattana, S., Rakkwamsuk, P. (2012). Effect of heat treatment on electrical properties of fluorine doped tin dioxide films prepared by ultrasonic spray pyrolysis technique. Procedia Engineering, 32, 663–669. doi: https://doi.org/10.1016/j.proeng.2012.01.1324
35. Memarian, N., Rozati, S. M., Elamurugu, E., Fortunato, E. (2010). Characterization of SnO2:F thin films deposited by an economic spray pyrolysis technique. Physica Status Solidi (c), 7 (9), 2277–2281. doi: https://doi.org/10.1002/pssc.200983738
36. Kim, H., Park, H.-H. (2012). A study on the electrical properties of fluorine doped direct-patternable SnO_2 thin films. Ceramics International, 38, S609–S612. doi: https://doi.org/10.1016/j.ceramint.2011.05.108
37. Ray, S. C., Karanjai, M. K., Dasgupta, D. (1997). Preparation and study of doped and undoped tin dioxide films by the open air chemical vapour deposition technique. Thin Solid Films, 307 (1-2), 221–227. doi: https://doi.org/10.1016/s0040-6090(97)00268-x